

Correlation of damage and analysis of R/C building: Experience from the 1995 Kobe earthquake

Taizo Matsumori† and Shunsuke Otani‡

*Department of Architecture, Graduate School of Engineering, The University of Tokyo,
7-3-1 Hongo, Bunkyo-ku, Tokyo 113-8656, Japan*

Abstract. During the 1995 Hyogoken-Nanbu Earthquake, a reinforced concrete building, called *Jeunesse Rokko*, suffered intermediate damage by forming a beam-yielding (weak-beam strong-column) mechanism, which has been regarded as the most desirable earthquake resisting mechanism throughout the world. High cost to repair damage at many beam ends and poor appearance expected after the repair work made the owner decide to tear down the building. Nonlinear earthquake response analyses were conducted to simulate the behavior of the building during the earthquake. The influence of non-structural members was considered in the analysis. The calculated results were compared with the observed damage, especially the location of yield hinges and compression failure of spandrel beams, and the degree of cracking in columns and in column-girder connections.

Key words: nonlinear response analysis; beam-yielding mechanism; shear crack; non-structural elements.

1. Introduction

It is generally accepted that the reinforced concrete frame building should be designed to form a total yield mechanism of beam-yield type (weak-beam strong-column mechanism) under earthquake forces. The followings have been pointed out to advocate the concept; i.e.,

- (1) The slender girder can easily develop large plastic deformation after flexural yielding because no axial force acts in the girder,
- (2) The hysteresis energy dissipation of the girder under load reversals in the inelastic range is stable and large,
- (3) Failure of a few girders will not lead to the collapse of the entire structure,
- (4) Ductility demand of individual girders is relatively small because the plastic deformation of the structure is distributed among many hinging girders, and
- (5) Significant kinetic energy of the structure can be dissipated in the form of hysteresis energy at many girder ends.

In addition, the flexural damage at girder ends was believed to be relatively easy to repair after a strong earthquake.

† Research Associate, M. Eng.

‡ Professor, Ph.D. and D. Eng.

A reinforced concrete building, called *Jeunesse Rokko*, drew the attention of structural researchers and engineers after the 1995 Hyogoken-Nanbu Earthquake. The building developed flexural yielding at ends of most girders and diagonal cracking in the column-girder connections and in the columns. The damage was generally judged to be moderate by structural researchers, but the owner decided to tear down the building because it was found expensive and difficult to rehabilitate the building maintaining its nice appearance of exposed concrete. A team of Arai-gumi Corporation, Kyoto University, Osaka University, Kinki University, and University of Tokyo jointly studied and recorded the damage of the building (Arai-gumi 1995).

In this paper, a series of nonlinear earthquake response analyses were conducted to simulate the damage of the building during the earthquake, and to correlate the observed structural damage and the calculated response by varying the modeling of non-structural members.

2. Building

2.1. Outline

The building was a 9-story reinforced concrete apartment building constructed in 1987. The building was located in Higashi-Nada Ward, one of the most heavily damaged areas in Kobe City. The structure consisted of two parallel moment-resisting frames in the longitudinal (north-south) direction with six uniform bays at 5.5 m; the number of bays was reduced to three in the 7th story and to two in the 8th and 9th stories. The structure has one span at 6.0 m in the transverse (east-west) direction. Total height of the building was 24.0 m. Story height was 3.0 m in 1st story, 2.625 m each from 2nd to 7th stories, 2.50 m in 8th story, and 1.50 m in 9th story. Structural elevations and a typical floor plan are shown in Figs. 1 and 2.

Surface soil was sandy soil with standard penetration test value (N-value) of 2 to 19, underlain by sand gravel layer (N-value of 26 to 50). Mat foundation was used after soil improvement of surface sandy soil.

The dimensions of columns were 800×900 mm in 1st story, and 700×700 mm in 6th and 7th stories. The dimensions of girders were 550×1700 mm in the foundation, 500×850 mm on 2nd floor, and 350×725 mm on 7th and 8th floors. Typical sections of columns and

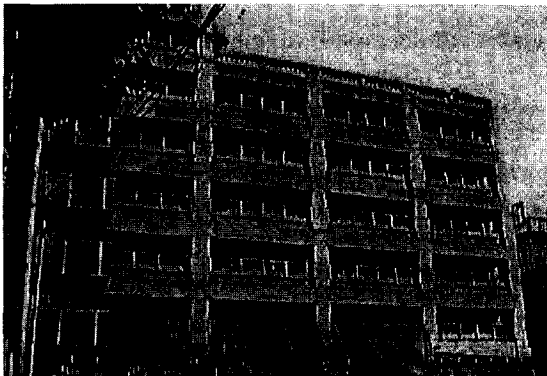


Photo. 1 East face (frame X_1)

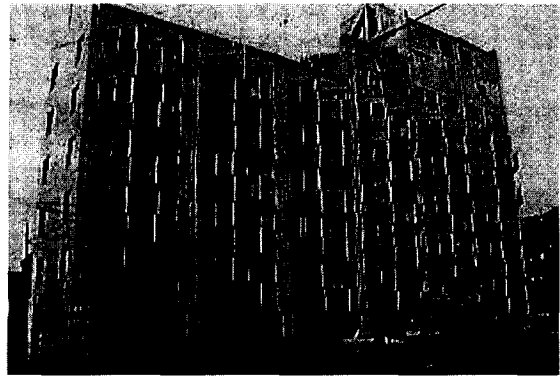


Photo. 2 West face (frame X_2)

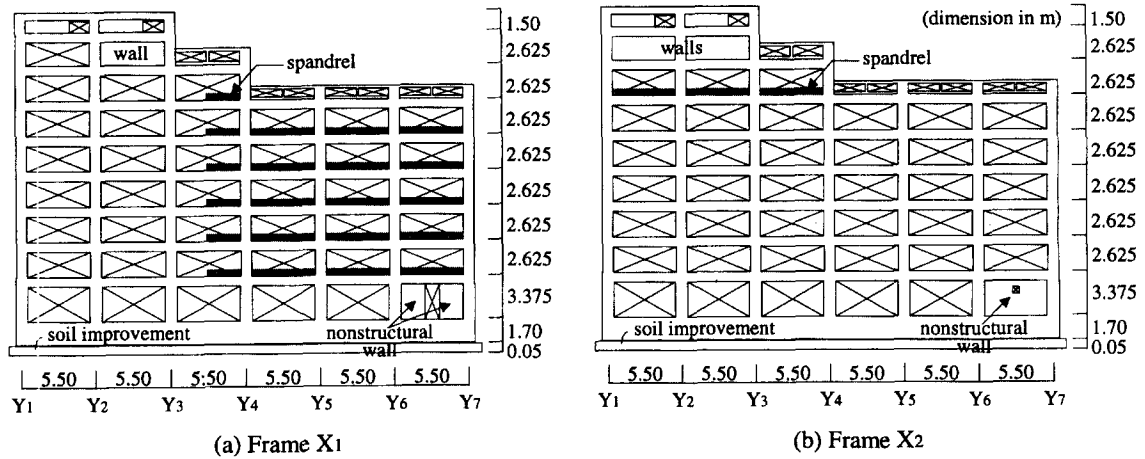


Fig. 1 Structural elevations

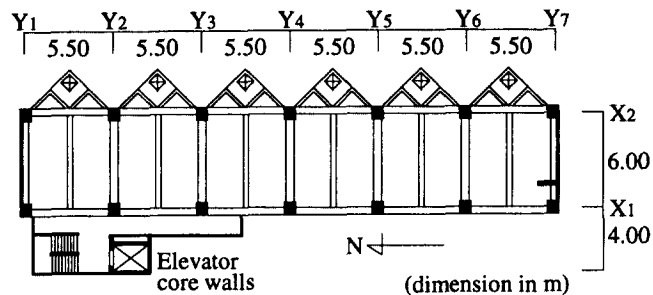
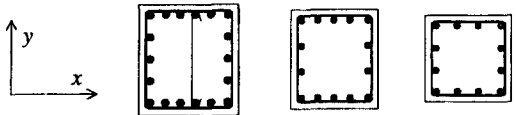
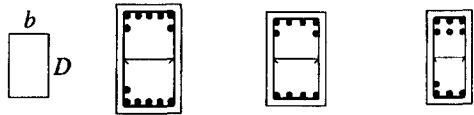


Fig. 2 Typical floor plan

girders are shown in Table 1. The thickness of floor slabs was 130 mm, except that the thickness of slabs was 150 to 175 mm in the corridor.

There were non-structural reinforced concrete walls (150 mm in thickness) in 1st story; the wall concrete was placed monolithically with boundary columns. These walls, however, were separated from the columns by embedded plastic tubes along the column face. Reinforced concrete spandrels (100 mm in thickness and 650 mm in height) were placed above 2nd to

Table 1 Typical sections of columns and girders

(a) Columns				(b) Girders			
Location	1st story	4th story	7th story	Location	2nd floor	5th floor	8th floor
$x \times y$	800 × 900mm	700 × 800mm	700 × 700mm	$b \times D$	500 × 850mm	450 × 725mm	350 × 725mm
Longi. bar	18-D29	14-D29	12-D25	Longi. bar	7, 6-D25	6, 4-D25	6, 4-D25
Hoop	D16@100mm	D13@100mm	D13@100mm	Hoop	D13@100mm	D13@150mm	D13@200mm
							
X ₁ /Y ₄ -column for each story				At ends of girders in the longitudinal direction			

7th floor girders in the longitudinal direction. A staircase and an elevator core were located in the northwest corner.

The exterior surface of transverse walls at south end was covered with tiles. The exterior surface of north-end walls was finished with exposed concrete. The apartment units were separated by autoclaved lightweight concrete partition walls.

2.2. Structural design

The structure was designed in accordance with the current Building Standard Law of Japan (revised in 1981).

The allowable stress design was carried out for gravity loads; the allowable stress of concrete was $(1/3)F_c$, and that of steel was $(2/3)F$, where F_c : nominal strength of concrete specified in design, and F : nominal yield stress of reinforcement. Design base shear coefficient in seismic design was 0.2; the allowable stresses were $(2/3)F_c$ and F . The story drift under the design seismic force must be less than 1/200 of the inter-story height.

The current building code requires the examination of lateral story shear capacity at the formation of collapse mechanism under lateral forces. The minimum story shear Q_{uni} for story i is defined as;

$$Q_{uni} = Z R_t D_s F_{es} C_o A_i W_i \quad (1)$$

in which, Z : seismic zone factor ($=1.0$ in Kobe City), R_t : vibration characteristic factor depending on soil condition ($=1.0$ for intermediate soil), D_s : structural characteristic factor ($=0.30$ for a structure consisting of ductile members), F_{es} : structural configuration factor ($=1.0$ for a structure of regular configuration in plan as well as along height), C_o : standard base shear coefficient ($=1.0$), A_i : factor representing vertical distribution of story shear coefficients, and W_i : vertical load above story i . The factor A_i is defined as

$$A_i = 1 + \left(\frac{1}{\sqrt{a_i}} - a_i \right) \frac{2T}{1 + 3T} \quad (2)$$

where $a_i = W_i/W_1$ and T : period of the structure ($=0.5$ sec).

2.3. Material properties

Nominal strength of concrete specified in design was 23.5 N/mm^2 from the base to 5th floor, and 20.6 N/mm^2 in the upper floor. Deformed D25 (cross sectional area $a_b=507 \text{ mm}^2$) and D29 ($a_b=642 \text{ mm}^2$) bars of grade of SD345 (minimum yield stress of 345 N/mm^2) were used as longitudinal reinforcement in columns and girders. Deformed D10 ($a_b=71 \text{ mm}^2$), D13 ($a_b=127 \text{ mm}^2$), and D16 ($a_b=199 \text{ mm}^2$) bars of grade of SD295 (minimum yield stress of 295 N/mm^2) were used as transverse reinforcement in columns and girders and also as reinforcement in walls and slabs.

Coupons of reinforcing bars and concrete cores were taken from the building during the investigation and were tested in the laboratory. Mechanical properties of concrete and steel are shown in Table 2. The compressive strength and Young's modulus of concrete are the average for each nominal strength. The yield stress of reinforcing bars was the average for each bar size. The material strengths were higher than the specified.

Table 2 Properties of materials

(a) Concrete			(b) Steel			
Nominal strength	σ_B	E_c	Size	σ_y	Size	σ_y
$F_c=23.5$ N/mm ²	29.5 N/mm ²	21.9 kN/mm ²	D13	361 N/mm ²	D25	358 N/mm ²
$F_c=20.6$ N/mm ²	28.5 N/mm ²	21.9 kN/mm ²	D16	330 N/mm ²	D29	368 N/mm ²

σ_B : compressive strength, E_c : Young's modulus σ_y : yield stress

3. Damage

Larger damage was observed in the longitudinal direction than in the transverse direction; a typical beam-yielding mechanism was formed with flexural crushing of concrete and wide crack openings at the ends of most girders. Crushing of concrete and buckling of reinforcing bars were observed at the top of spandrel ends. X-shaped shear cracks were observed in many columns and column-girder connections especially on the exterior sides. Outline of the damage is shown in Fig. 3.

3.1. Girders and spandrels

Flexural crushing of concrete and wide crack openings were observed at the ends of most girders at every floor level. Typical damage is shown in Photo. 3. The width of cracks was 0.2 to 1.4 mm at the ends, and 0.2 to 2.0 mm in the mid-span. Flexural cracks narrower than 0.1 mm were also found in transverse beams. All of the reinforced concrete spandrel beams placed on 2nd to 6th-floor girders were crushed at the ends adjacent to the columns; reinforcing bars were exposed and buckled. The spandrel beams on 7th-floor girders, on the other hand, were found to suffer slight damage.

3.2. Columns

X-shaped shear cracks were observed in many columns in the longitudinal direction on the exterior sides. Damage level of the columns was shown in Table 3. The damage levels were classified as follows:

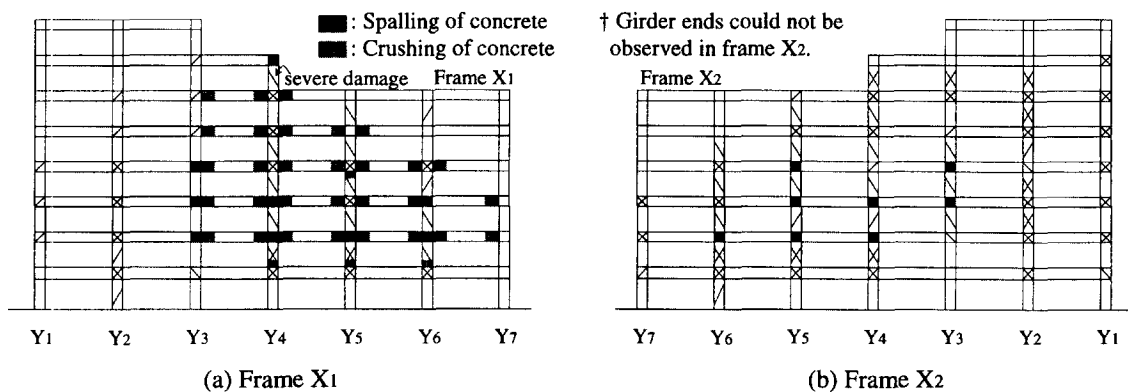


Fig. 3 Distribution of damage in longitudinal frames

Table 3 Damage level of columns

Story	Number of total columns	Number of observed columns	Damage level					
			0	I	II	III	IV	V
8	6	3	3	0	0	0	0	0
7	8	8	2	0	1	1	4	0
6	14	14	7	2	2	3	0	0
5	14	14	4	2	6	2	0	0
4	14	14	3	3	6	1	1	0
3	14	14	2	4	7	1	0	0
2	14	14	1	5	3	4	1	0
1	14	14	6	4	3	0	1	0

- "0" : no structural damage,
 "I" : flexural cracks at the top or the base of column,
 "II" : shear cracks narrower than 1 mm,
 "III" : shear cracks of about 2-mm width and some spalling of concrete,
 "IV" : wide shear cracks exposing reinforcement, and reduction in shear resistance of columns,
 "V" : crushing of concrete and buckling of reinforcement, and reduction in axial load carrying capacity.

The damage of columns was moderate between 2nd and 6th stories; the damage was severest in the 2nd story. The damage of columns from Y_4 to Y_6 in X_1 frame, to which the spandrel beams were connected, was classified as "III" or "IV". Shear cracks opened wider on the exterior face than on the interior face because the girders were connected eccentrically to the exterior face of the columns. The width of shear cracks was 0.2 to 2.0 mm on the exterior face, and about 0.2mm or less on the interior face.

The damage was relatively light in the 1st story; the damage level of all the columns except for X_1/Y_2 -column was "0", "I", or "II". The damage of X_1/Y_2 -column was classified as "IV"; X-shaped shear cracks opened wide and a lateral reinforcing bar were found to rupture. Because severe damage was not observed in any other columns in the 1st story, the damage of X_1/Y_2 -column may have been caused accidentally attributable to low quality of materials or construction work. The damage was severe in the 7th story; four columns out of eight columns were classified as damage level "IV" (Photo. 5). Deformable length of these columns was shortened by the spandrels. The damage was hardly observed in 8th and 9th story columns.

3.3. Column-girder connections

X-shaped shear cracks were observed in many interior girder-column connections in the longitudinal direction (Photos. 3 and 4). The damage was relatively severe between 3rd- and 5th- floor column-girder connections; the width of shear cracks was more than 2 mm, and the spalling of concrete was also observed. The damage was lighter in the connection at X_1/Y_2 than in the other interior connections of the same floor. Shear cracks on the exterior face were wider than those on the interior face; the girders were connected to columns eccentrically at the outer face, and the transverse beams were connected inside of the connections.

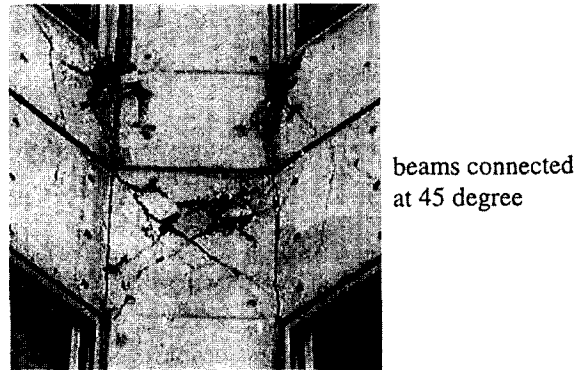
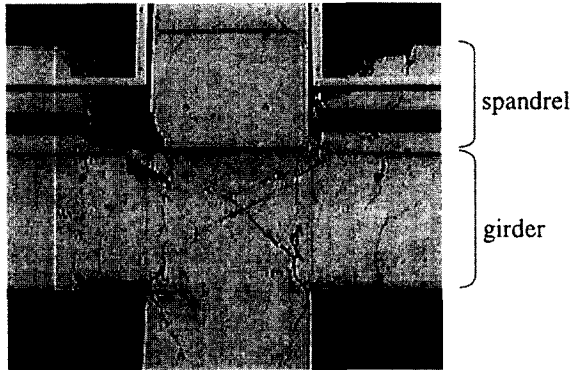


Photo. 3 Column-girder connections in frame X_1 Photo. 4 Column-girder connections in frame X_2

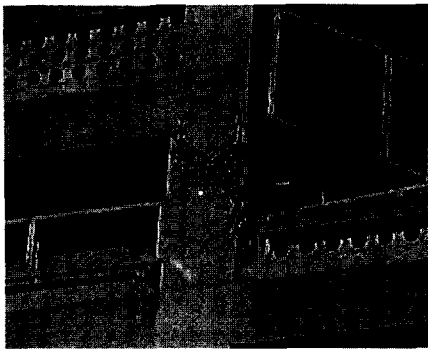


Photo. 5 Seventh-story column



Photo. 6 Non-structural wall in first story

3.4. Non-structural walls

Many shear cracks were observed in the non-structural walls in the 1st story. These walls were separated from the structure by plastic tubes embedded along the column face; nevertheless, large lateral force must have been acted on these walls. Sliding shear failure was observed in the wall between Y_6 and Y_7 of frame X_2 ; the reinforcing bars were partially exposed on both sides of the opening (Photo. 6). The damage in elevator core walls, typically flexural cracks, was concentrated in the 1st story.

4. Method of response analysis

A series of nonlinear earthquake response analyses were carried out in the longitudinal direction using an observed earthquake ground motion record.

4.1. Modeling of structure

The structure was idealized as two plane frames. Floor slabs were assumed to be rigid in their own plane, causing two frames to have the same horizontal displacements at each floor. The frames were assumed to be fixed at the base. The mass of the structure was assumed to

be concentrated at each floor level. The effect of torsion and transverse frames was ignored.

A girder and column were idealized as an elastic linear element with two nonlinear rotational springs at the ends (Fig. 4). Axial deformation was considered in the elastic element of a column member. Column-girder connections were assumed to be rigid (Fig. 5). Structural walls in 8th and 9th stories were modeled by an equivalent column with rigid boundary girder (Fig. 4).

The effect of non-structural elements on the earthquake response was studied in five cases (Table 4). The non-structural walls in the 1st story were modeled by an equivalent column with rigid boundary girders (Fig. 6). The slender walls around the elevator core were idealized as three equivalent columns connected to the two frames at each floor level.

Table 4 Modeling of non-structural elements

Members	Case A	Case B	Case C	Case D	Case E
Non-structural walls in 1st story	x	o	x	o	o
Walls around elevator core	x	x	o	o	o
Spandrels	x	x	x	x	o

x: ignored in the analysis, o: considered in the analysis

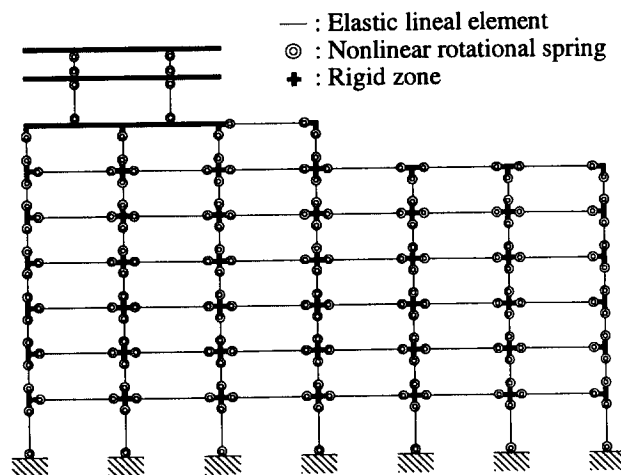


Fig. 4 Modeling of frame (Case A)

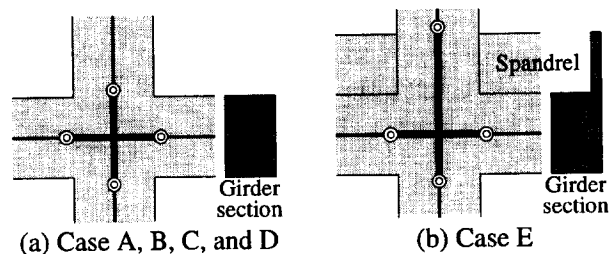


Fig. 5 Modeling of girder-column connections

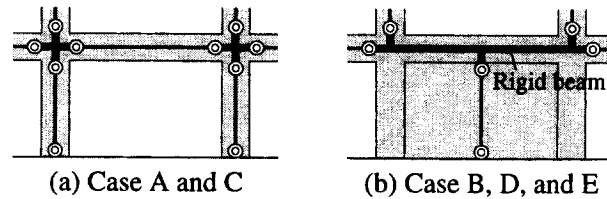


Fig. 6 Modeling of 1st-story walls

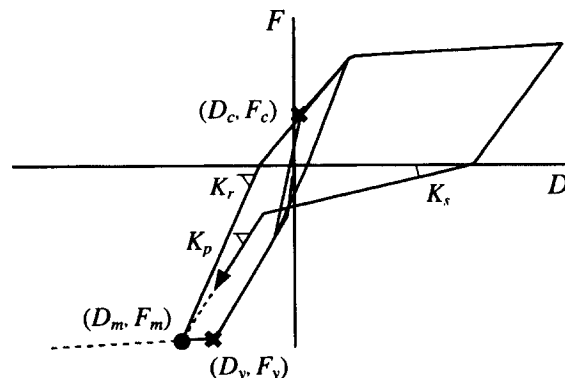
4.2. Force-displacement relationship of members

Force-displacement relationship of a member was evaluated using measured dimensions and observed material properties (Table 2). Elasto-plastic relation was assumed for reinforcement; a parabolic curve up to 0.002 strain followed by linear descending relation was assumed for concrete.

The moment-curvature relation was represented by a tri-linear relation with stiffness changes at flexural cracking and yielding. The elastic stiffness was evaluated for concrete sections ignoring contribution of reinforcement. Girders were analyzed as T-shaped section considering cooperative slab width of 0.1 times span length. Flexural cracking and yielding moments were computed using stress-strain relationship of materials, equilibrium of forces and linear strain distribution.

Member end rotation for a column and girder was evaluated assuming linear curvature distribution along the member with zero curvature at mid-span. Member end rotation of a wall was evaluated for uniform curvature distribution. The stiffness after yielding was taken 1.0% of the initial elastic stiffness. The reduction in resistance of a spandrel beam after compression failure was not considered. The curvature at the maximum flexural resistance of a girder with a spandrel beam was approximately 1.25 times the curvature at flexural yielding.

The Takeda-slip hysteresis model (Otani *et al.* 1984, Fig. 7) was used in the moment-rotation relationship at each member end. The values of slipping stiffness degradation parameters γ were 1.0 for negative bending of the girders, and 0 for the other members. The value of slipping stiffness degradation parameter η , and unloading stiffness degradation parameter α was 1.0 and 0.4 respectively.

Fig. 7 Takeda-slip hysteresis model (Otani *et al.* 1984)

Shear deformation was assumed proportional to flexural deformation for columns and girders. Shear deformation was ignored for slender elevator core walls. The shear force-deformation relation of a wall was represented by a tri-linear relation with stiffness changes at shear cracking and yielding. The initial elastic stiffness K_s was calculated by Eq. (3):

$$K_s = \frac{GA_w}{\kappa h} \quad (3)$$

in which G : elastic shear modulus, A_w : area of shear wall section, h : inter-story height, and κ : shape factor for shear deformation. Shear cracking was assumed to occur when the average shear stress in a wall panel exceeded the tensile strength of concrete given by $0.44(\sigma_B)^{1/2}$ N/mm², where σ_B was the compressive strength of concrete in N/mm². Shear yielding strength Q_{su} (N) was evaluated by the empirical equation (Hirosawa 1975) as follows:

$$Q_{su} = \left[\frac{0.0679p_t^{0.23}(\sigma_B + 18)}{\sqrt{M/QL + 0.12}} + 0.85\sqrt{\sigma_{wh}p_{wh}} + 0.1\sigma_0 \right] b_e j \quad (4)$$

where p_t : effective tensile reinforcement ratio (%) = $100a_t/\{b_e(L - D/2)\}$, a_t : area of longitudinal reinforcement in a tensile boundary column (mm²), M/QL : shear-span-to-depth ratio, σ_{wh} : yield strength of horizontal reinforcement (N/mm²), p_{wh} : effective horizontal wall reinforcement ratio = $a_{wh}/b_e x$, x : spacing of horizontal reinforcement (mm), σ_0 : average axial stress over entire wall cross sectional area (N/mm²), b_e : average width of wall section (mm), $j = (7/8) \cdot (L - D/2)$ (mm), L : total depth of wall section (mm), and D : depth of compression-side boundary column section (mm). The ratio of secant stiffness at shear yield point to the elastic stiffness was empirically determined to be 0.16. The stiffness after shear yielding was taken 0.1% of the initial elastic stiffness. An origin-oriented hysteresis model was used in shear force-deformation relationship for walls.

4.3. Response computation

The earthquake accelerogram used in the analysis was the N30W record (Fig. 8) measured at Fukiai Osaka Gas Station, located in the most heavily damaged area and about 3 km to the west of the building. The maximum acceleration was 8.02 m/s².

A damping was assumed to vary proportional to the instantaneous stiffness. The first mode damping factor was assumed to be 5% at the initial elastic stage.

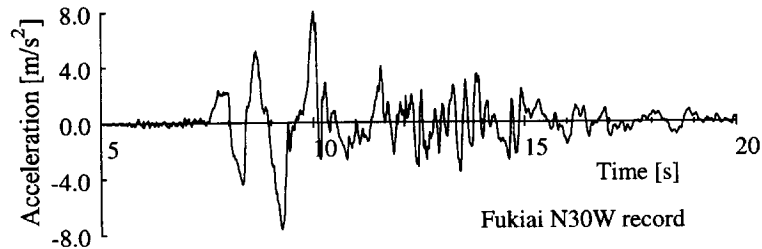


Fig. 8 Input accelerogram

5. Analysis results

5.1. Response waveform

Calculated response waveforms of base shear coefficient (base shear divided by the entire weight) and roof drift (the roof-level displacement divided by the overall height) for Cases A (no non-structural members) and D (with non-structural walls) are compared in Figs. 9 and 10. The base shear coefficient response waveforms (Fig. 9) are generally similar for the two cases, and the peak amplitudes exceeded 0.4 in two cycles followed by relatively small signals after 10.5 sec. The large amplitude response of the two cases corresponded to large spikes in the base motion (Fig. 10). The base shear response of Case D contained short period components in the latter part of the response compared with the response of Case A.

The two analytical models exhibited a significant difference in the roof-drift waveforms (Fig. 10). The roof drift of Case A exceeded 2.0 percent, while the roof drift of Case D reached only 0.85 percent. The non-structural walls (Case D) added significant stiffness to the structure. Displacement response was dramatically reduced by the non-structural walls.

The base shear coefficient-roof drift relations of Cases A and D are compared in Fig. 11. The pure frame model (Case A) developed yielding at base shear coefficient of 0.4, and large inelastic deformation took place in the large amplitude oscillation.

5.2. Maximum story drift

Maximum story drifts (inter-story displacement divided by the inter-story height) are shown in Fig. 12. Largest story drift was calculated for Case A; story drifts over 3.0% were calculated from 1st to 4th stories. The modeling of non-structural walls in the 1st story in Case B, the story drift was reduced much from Case A (pure frame model) especially in 1st

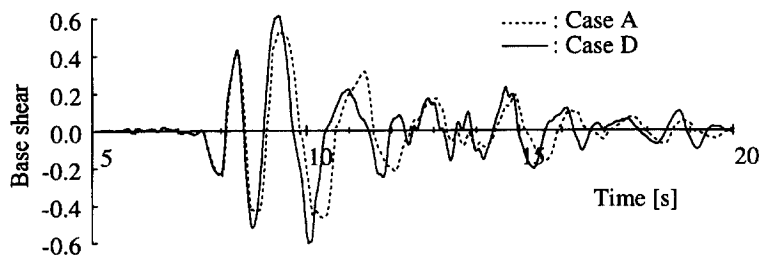


Fig. 9 Response base shear

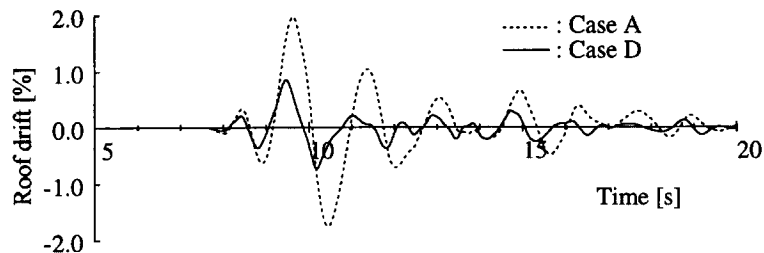


Fig. 10 Response roof drifts

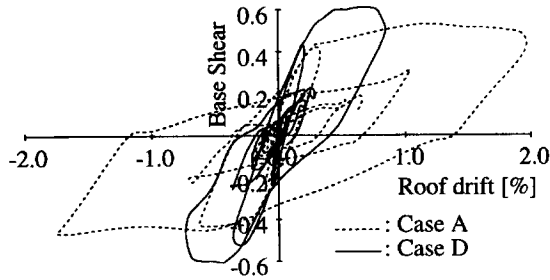


Fig. 11 Base shear-roof drift relations

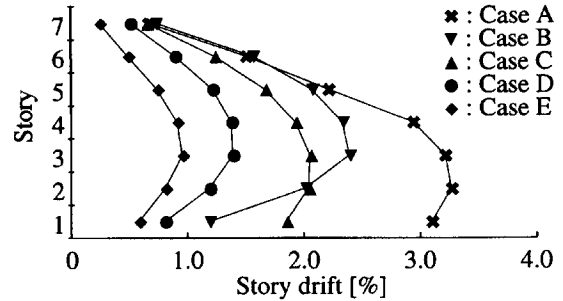


Fig. 12 Maximum response story drifts

and 2nd stories; maximum story drifts were reduced to 38% and 62% of Case A in 1st and 2nd stories, respectively. By including the elevator core walls in the analysis of Case C, story drifts were reduced at 1st to 4th stories; maximum story drifts were reduced to 60 to 66% of Case A in these stories. If both 1st-story non-structural walls and the elevator core walls were considered in Case D, story drifts were significantly reduced to 26% and approximately 40% of Case A in the 1st story and from 2nd to 4th stories, respectively. The effect of monolithic non-structural walls is significant on the deformation response of a building.

5.3. Formation of flexural yielding

The formation of yield hinges is compared for Cases A, D and E in Fig. 13; the location of compression failure in spandrel beams is also indicated for Case E. In all three cases, the structure developed flexural yielding at all girder ends from 2nd to 7th floors, at the base of 1st-story columns and at the top of 7th-story columns. In Cases B and D with non-structural walls in the 1st story, yield hinges were also calculated at the base of 2nd-story columns; the non-structural walls in the 1st story yielded in shear. In Cases C and D with elevator core walls, the walls yielded in flexure at the base of 1st and 2nd stories.

In Case A, the structure formed the yield mechanism in an early stage of the ground motion due to the lack of horizontal resistance; rotational ductility demand reached as large as 10.0 at the girder ends from 2nd to 4th floors and at the 1st-story column bases. In Case D, rotational ductility demand was around 4.0 at the girder ends in 2nd to 6th floors.

When the spandrel beams were considered in Case E, girder-end ductility demand was reduced to 1.6 to 2.5 in the positive bending at the ends of 2nd to 6th-floor girders; the response was large enough to cause failure of the spandrels. Bending moment in the 7th-floor girders was, however, less than the flexural yielding moment in the positive bending. Flexural yielding was calculated at the base of 2nd-story columns at Y_6 and Y_7 in frame X_1 .

The locations of flexural yielding and the amplitude of girder-end ductility demand agreed favorably with the observed damage for Case D, including the degree of flexural crushing of concrete at girder ends and at 2nd-story column bases, the extent of flexural cracking in the 1st-story walls around the elevator core, and slipping shear failure of the non-structural walls in the 1st story. Crushing of spandrels observed from 2nd to 6th floors, but not at the 7th floor, could be explained by the analysis of Case E. In the following discussion, the simulation of damage by Cases D and E are considered.

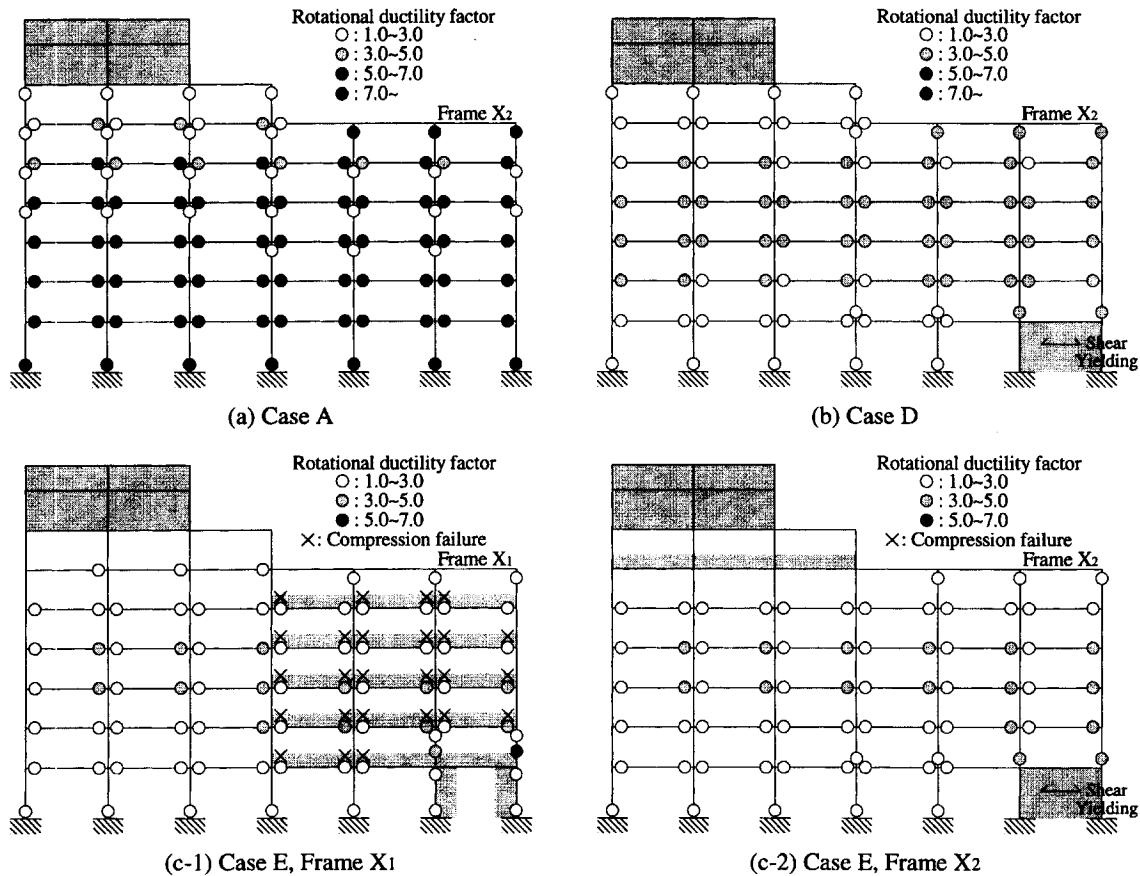


Fig. 13 Location of yield hinges and compression failure of spandrels

5.4. Column damage in shear

Shear forces in columns calculated for Cases D and E are compared with shear cracking strength in Table 5. Columns connected to spandrels are shown in shade in Table 5. Shear cracking strength Q_c (N) was calculated by using the empirical equation (Arakawa 1970) as follows:

$$Q_c = \frac{0.0612(\sigma_B + 50)}{M/QL + 1.7} bj \quad (5)$$

where σ_B : compressive strength of concrete (N/mm²), M/QL : shear-span-to-depth ratio, b : width of section (mm), and j : distance between top and bottom bars (mm). The equation was derived for 1,200 beam specimens to give mean shear cracking strength.

In Case D, calculated forces exceeded the shear cracking strength in 1st and 2nd stories, and were comparable to the shear cracking strength from 3rd to 7th stories. Case D was reasonably well in simulating the observed shear cracking in the columns from 2nd to 6th stories. However, the analysis failed to explain minor damage observed in the 1st story and shear failure of the columns in the 7th story.

Table 5 Ratios of calculated shear to shear cracking strength in columns

	Location	Story					
		1	2	3	4	5	7
Case D	X ₂ Y ₂	1.39	1.55	1.14	1.01	1.18	0.83
	X ₁ Y ₅	1.30	1.49	1.19	1.05	0.98	1.07
Case E	X ₂ Y ₂	1.54	1.20	1.10	0.95	1.02	0.80
	X ₁ Y ₅	1.30	1.63	1.29	1.23	1.20	1.16

Columns connected to spandrels are shown in shade

When spandrels were considered in Case E, column shear forces increased to favorably explain severer damage observed in 2nd- to 6th-story columns connected to the spandrels. In the 2nd-story columns at X₁/Y₆ and X₁/Y₇ above the 1st-story non-structural wall, large shear forces were calculated exceeding the ultimate shear strength due to the stiffening effect attributable to the support of the columns by rigid girders and to the shortening of deformable length of the columns by the spandrels.

5.5. Shear cracking in column-girder connections

Shear forces in column-girder connections calculated for Cases D and E are compared with shear cracking strength in Table 6. Shear V_j in a column-girder connection (Fig. 14) was calculated by Eq. (6):

$$V_j = T_l + T_r - \frac{1}{2} (V_{cu} + V_{cl}) \quad (6)$$

where T_l , T_r : tensile forces in girder reinforcement, calculated from girder moment at column faces, and V_{cu} , V_{cl} : shear force in the upper and lower columns. A column-girder connection was assumed to crack in shear when the principal tensile stress exceeded the tensile strength of concrete.

The calculated shear was comparable to the shear cracking strength in all the interior column-girder connections simulating favorably the observed shear cracks in the interior column-girder connections. The ratios of the calculated shear to the shear cracking strength were slightly smaller at X₁/Y₂ than at X₁/Y₅ in each floor. The calculated shear in X₁/Y₂-connection was comparable to that in X₁/Y₅; larger axial force acted in X₁/Y₂-connection than

Table 6 Ratios of calculated shear to shear cracking strength in column-girder connections

	Location	Floor				
		2	3	4	5	7
Case D	X ₁ Y ₂	0.99	1.24	1.14	1.07	0.99
	X ₁ Y ₅	1.10	1.36	1.22	1.22	1.12
Case E	X ₁ Y ₂	0.98	1.24	1.09	1.04	0.96
	X ₁ Y ₅	1.02	1.14	1.00	0.96	0.82

Column-girder connections connected to spandrels are shown in shade

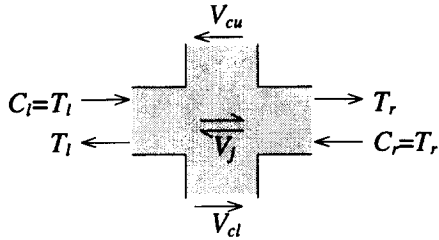


Fig. 14 Shear in column-girder connection

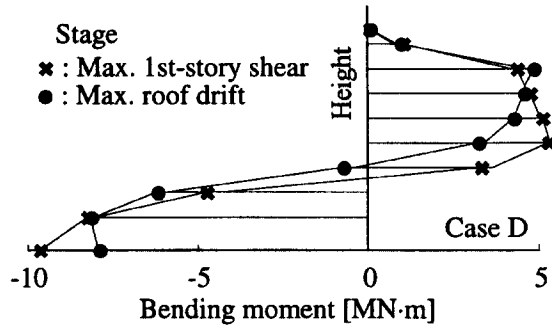


Fig. 15 Bending moment in the elevator core walls

Table 7 Ratios of calculated shear in non-structural elements to first-story shear

Stage	First-story walls	Elevator core walls
Elastic stage	0.41	0.20
Maximum story shear	0.38	0.028

in X_1/Y_5 -connection.

In Case E with spandrel beams, the calculated shear was smaller than the cracking shear strength because shear was larger in the columns connected to the spandrels. The reduction in column shear with flexural crushing of spandrel beams increased the shear in the connections and caused shear cracking.

5.6. Effect of non-structural elements

The ratios of shear in the 1st-story walls and the elevator core walls to the 1st-story shear calculated for Case D are shown in Table 7.

5.6.1. First-story walls

Shear force in the 1st-story walls was as large as 41% of 1st-story shear at the elastic stage. The ratio decreased with shear cracking in the wall, but the ratio started to increase to 33% after the flexural yielding at the base of 1st-story columns until shear yielding in the wall. The non-structural walls have large effect on the resistance in the 1st story. The non-structural walls should be clearly separated from the structural elements to avoid the ill contribution.

5.6.2. Elevator core walls

Shear force in the elevator core walls was as large as 20% of the 1st-story shear at the elastic stage. The ratio decreased as the region of flexural yielding spread from the base to the top in the 1st story; decreased to 2.8% when the 1st-story shear reached maximum. Bending moment in the walls is shown in Fig. 15 for Case D. The inflection point was located near the base of 4th story. The walls carried large shear only in 3rd and 4th stories where story drift was largest. The ratios of shear in the walls to story shear were 25% in 3rd story, and 16% in 4th story at the maximum roof-level response displacement.

5.6.3. Spandrel beams

When the spandrels were considered in Case E, the beam end rotation was reduced and column shear was increased at the connection to the spandrels. Because the dimensions of spandrels were the same on all floors, the reduction of girder-end ductility due to the stiffening effect of spandrels was large in the upper stories where the dimensions of girders were smaller. However, the change in the effective length of columns and girders with the deterioration of the spandrels could not be modeled in the present study.

6. Conclusions

The following conclusions may be drawn from the study;

1) Nonlinear earthquake response analysis must include reinforced concrete non-structural elements if they are constructed monolithically with the structural members.

2) Considering the non-structural walls in the analysis, the locations of flexural yielding at girder ends, shear cracking in columns and shear cracking in beam-column connections could be simulated favorably by the analysis. The shear failure of columns in the 7th story was not reproduced by this analysis.

3) By additional consideration of spandrels in the analysis, shear in the columns adjacent to the spandrels increased, but the shear in the beam-column connections decreased. Further study is needed to model the change in deformable length of members with propagation of damage in the spandrels.

References

- Arai-gumi Technical Research Department (1995), "Damage investigation report on the 1995 Hyogoken-Nanbu Earthquake -Jeunesse Rokko- (in Japanese)", *Technical Research Report*, **8**, Arai-gumi, 221.
- Otani, S., Kabeyasawa, T., Shiohara, H., and Aoyama, H. (1984), "Analysis of the full scale seven story reinforced concrete test structure", *ACI SP 84-8*, 203-239.
- Hirosawa, M. (1975), "Past experimental results on reinforced concrete shear walls and analysis on them (in Japanese)", *Kenchiku Kenkyo Shiryo*, **6**, Building Research Institute, Ministry of Construction.
- Arakawa, T. (1970), "Allowable unit shearing stress and design method of shear reinforcement of reinforced concrete beams, -Analysis of existing test data- (in Japanese)", *Concrete Journal*, **8**(7), 11-20.